ATLAS SCT Commissioning – TWEPP-08

C.A Magrath[a], on behalf of the ATLAS SCT collaboration

[a] Radboud University, Nijmegen, The Netherlands

cmagrath@nikhef.nl

Abstract

The Barrel and Endcaps of the ATLAS SemiConductor Tracker have been installed in the ATLAS cavern since summer 2007. All the electrical and optical services were connected and rapid tests performed to verify their continuity. Problems with the cooling circuits, meant that the time for detailed tests in 2007 was limited. These problems have now been resolved allowing the SCT to be operated and participate in combined ATLAS Cosmic ray data taking runs. The results of these runs have been used to determine the hit efficiency of the modules as well as providing invaluable constraints for the detector alignment.

I. INTRODUCTION

One of the largest and most carefully designed particle detectors of our time is the ATLAS detector [1]. Every 25 ns at the LHC [2] a proton-proton interaction will occur, with a centre of mass energy of 14 TeV. Momentum and vertex resolution requirements are of key importance throughout the experiment, hence meticulous measurements are needed. The inner detector (ID) [1] is housed within the central solenoid which provides a magnetic field of 2T to the ID. A detailed system of different types of detectors are necessary in order to accommodate the large density of tracks anticipated at the LHC. There are three sub-systems associated with the ID: Pixels, Semi-Conductor Tracker (SCT) and the Transition Radiation Tracker (TRT). Figure 1 shows a schematic of the ID, with specifics given for the SCT. The details of the silicon tracker will now be discussed.

A. Silicon Tracker Design and Layout

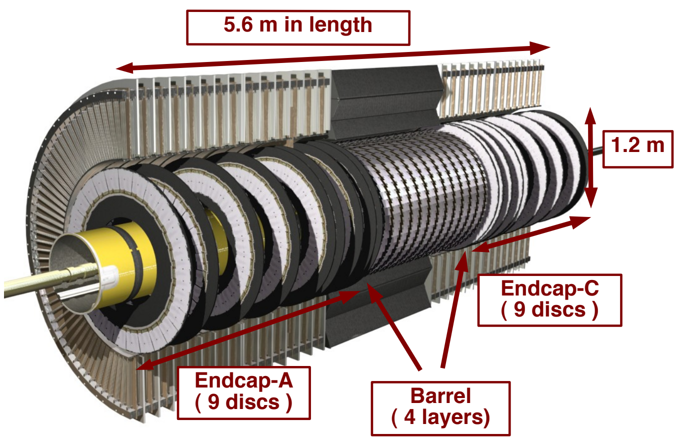

Figure 1: The Inner Detector, with details of the Semi-Conductor Tracker.

The Semi-Conductor Tracker is positioned as the second closest to the point of interaction. It comprises 4 central barrels and two end-caps, each with nine discs. The basic element of the system is the module. The SCT itself occupies a radial region between 25 and 50 cm. Its design provides 4 space point measurements for a particle originating from the interaction point, up to a pseudo-rapidity coverage of $\eta \geq 2.5$. In total the SCT has an active silicon area of 61 m^2. Silicon micro-strip technology provides fine granularity, which in turn, is central to the momentum, impact parameter and vertex position measurements.

B. Module Design and Operation

There are 4088 modules, equating to 15912 silicon strip wafers in the SCT. The barrel section has 2112 modules with only one module type [3], whilst each end-cap has nine discs populated with trapezoidal modules [4]. A detector module consists of gluing two pairs of single sided sensors, back to back on a highly thermally conducting substrate. There is a small stereo angle of 40 mrad between each side. Each end-cap has four module types Outer, Short Middle, Middle and Inner containing a combination of five wafer types. Each sensor is read out by Application Specific Integrated Circuits (ASICs) [6], incorporated on the detector module itself. They consist of a front-end amplifier and discriminator and a binary pipeline to store the hits. Each module side is served by 6 of these chips, each one responsible for 128 read-out channels.

A particle traversing the detector induces a current in a strip. The generated current signal is amplified and a voltage output fed into the main amplifier known as the shaper. It provides the pulse shaping according to the timing requirements and it filters the noise in order to maximise the signal to noise ratio, S/N. It detects the presence of a signal when the amplitude is above a pre-defined threshold. When the signal is above this threshold, a 1 is registered and when it is below a 0 is returned. In this way, hit or no hit information is provided and is stored for each of the 128 channels of the chip.

It is extremely important that the charge induced on the aluminium strips is understood. Attention must be given when setting the threshold such that the noise is kept to a minimum, whilst the efficiency is maximised. The maximum allowed noise during the initial LHC start-up, with sensor temperatures $\sim -7^\circ$ C, is set at 1500 ENC, increasing to 2000 ENC during the end of the detector lifetime. With these specifications , this gives an efficiency better than 99% and a noise occupancy less than 5×10^{-4}. Finally, during the module production, a limit of 1% of the module channels are allowed to be defective.

C. Optical Communication and Readout

Optical links are used to transfer the data from the modules off-detector, as well as distributing the bunch crossing clock, level 1 triggers and commands to the modules [7]. The entire SCT system uses 8176 data links and 4088 transmission links. Vertical Cavity Surface Emitting Lasers (VCSELs) are used for transmission of light signals, and epitaxial Si p-i-n diodes for the receiving of light signals. For each module, two data links and one Timing, Trigger and Control link exist, and are housed in a light tight package. The data links are operated at 40 Mbit/s, transferring data from the modules off the detector. Single bit errors as well as random hits will cause a loss in the number of real hits being read out. An upper limit of 10^{-9} for the bit error rate (BER) is set in order to maintain a high level of working efficiency for the optical links. The optical links used for the read-out of each module have undergone various stages of testing to ensure that they meet the requirements set out by SCT.

D. Installation and Commissioning

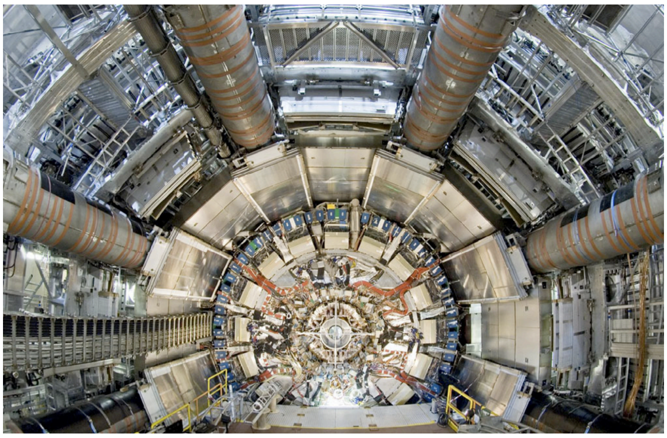

Figure 2: The ATLAS ID Endcap after complete insertion within the Liquid Argon Cryostat, May 2007.

By the summer of 2007 the SCT barrels and endcaps were successfully installed in the ATLAS cavern. All optical and power connections to the modules have been tested and most faults repaired. The electrical tests of barrel modules were initially delayed due to cooling problems. This caused a substantial delay in the time allowed for sign-off tests and further commissioning. In March 2008 the SCT barrel participated in its first "'Milestone" run, M6. Within hours, cosmic rays were tracked within the detector. Since then, both endcaps have been signed off, but further problems with cooling have delayed any further participation in combined ATLAS commissioning runs. The cooling problems and solutions will be discussed further on in this note.

II. Detector Performance

The modules as well as the support structure and services were built at the collaborating institutes. The final assembly of the SCT barrel was performed at Oxford University. Endcap-A was assembled at NIKHEF (Amsterdam), whilst Endcap-C was assembled at Liverpool University. At every stage of the assembly chain, the modules and services were extensively tested. At production sites, the components were tested before being sent to one of the assembly sites for the construction of the barrel or endcap detectors. Four main stages of tests can be considered:

- Disc/barrel assembly
- Macro-assembly
- Surface reception tests
- Cavern tests

Initially the optical settings for the module communication were set before proceeding with testing the analogue and digital aspects of the module chips. The digital tests check that the redundancy links between modules are functional, the chips bypass links are tested as well as a test of the pipeline circuitry. The analogue measurements include calculating the gain, offset and input noise for each module channel. The performance results over these last two years will now be summarised.

A. Optical links

To allow for a stable data communication between the modules and the readout acquisition, the optical settings for the readout must be optimised. Various tests have been carried out to ensure the best working set-up with regards to sending data to and from the modules. It is also an important factor that the links can work over a wide range of settings. Each RX optical link needs to have the receiver threshold correctly set so that there will be no loss in valid hits from the detector. Analyses of the optical links performance have been performed for barrels and endcaps by calculating the working range of each link. In total, more than 98.7% of the links on Endcap-A were fully functional, 99.5% on Endcap-C and 99.4% on the Barrel. VCSELs which were either declared dead or too problematic to read out data were recovered via the redundancy scheme.

B. Leakage Currents

Module sensors were manufactured by both Hamamatsu and CiS [5]. The modules produced by the latter suffered from an earlier onset of micro-discharge and higher leakage currents. This was as a result of using the non-field plate strip configuration (where the metal strip is narrower than the width of the p-implant.) The barrel modules only used Hamamatsu wafers, therefore they did not suffer from this early micro-discharge effect.

Figures 3,4 show a typical I-V curve for a Hamamatsu and CiS module. The different field plate geometries are reflected in the results. A measurement was taken of all the modules in the ATLAS cavern. The measurements were repeated several times allowing the current to settle, before being ramped to the next voltage. On average barrel modules had leakage currents of ∼150-500 nA and endcap modules between ∼200-1000 nA at room temperature. There were 6% of barrel modules (127) and 3% of endcap modules, which were unresponsive to any bias application. These problems are in the process of being investigated.

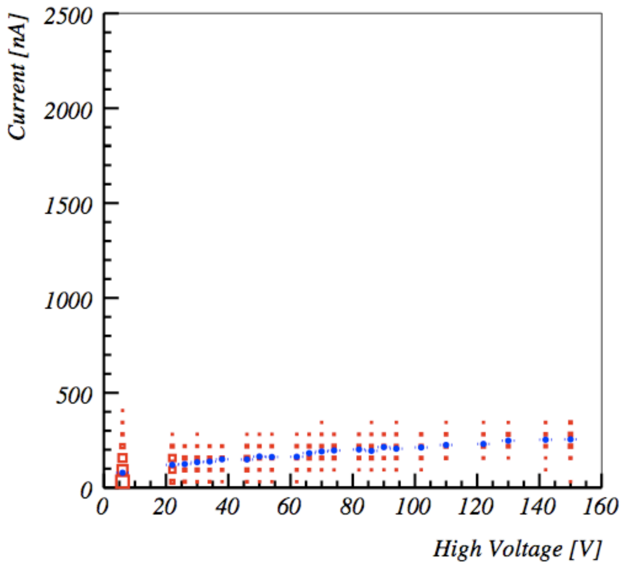

Figure 3: A typical I-V scan for a Hamamatsu sensor that uses the field-plate geometry.

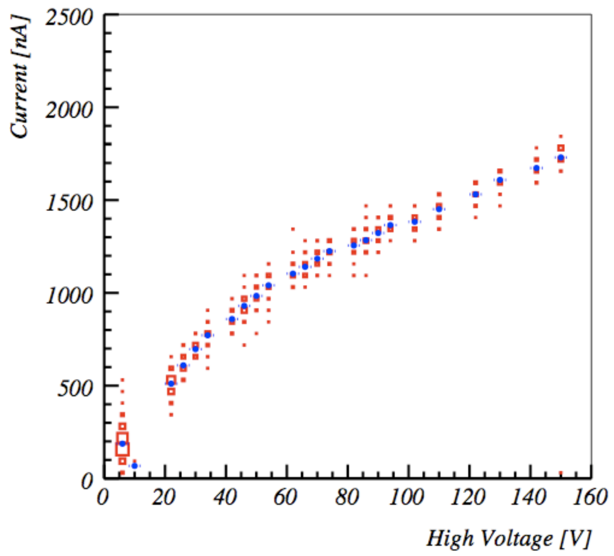

Figure 4: The CiS module shows higher leakage currents during an I-V scan due to the use of a non-field plate geometry.

C. *Input Noise*

A 3Pt-gain test [10] was the quickest form of testing the module to see that it was well within the specifications for input noise and channel efficiency. The scan determines the input noise using the gain, 50% occupancy threshold point and offsets for each module. A list of all the defective channels is also determined. In total 3897 strips were defective for Endcap-A, with a similar number for the barrel modules. This gives an efficiency of more than 99.7% of working strips. If a module has not been trimmed properly, then the input noise of the scan will show this, since the variation from channel to channel is noticeable.

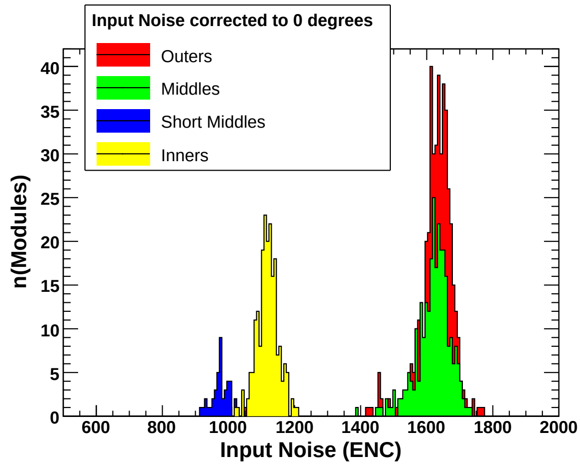

Figure 5: The distribution of the input noise during tests in the ATLAS cavern for Endcap-A.

Depending on the module type, the input noise level will vary accordingly. For barrel modules, the input noise should be similar for, since the geometry is the same for all. For the end-caps, the different module geometries must be considered. For inner and short-middle modules that consist of only one sensor on each module side, the length of the module strip is much shorter than an outer or middle module. This results in the noise at the input to the amplifier being lower. Figure 5 shows the spread in the input noise for each module group for data taken in the ATLAS cavern for Endcap-A. The data has been normalised to a module temperature of 0°C .

Test Stage	OUTER	MIDDLE	SH-MIDDLE	INNER
Disc	1608± 51	1532± 45	928± 26	1070± 32
Cylinder	1589± 52	1529± 46	929± 25	1066± 33
SR1	1592± 77	1568± 62	932± 39	1082± 45
Cavern	1622± 83	1620± 51	977± 26	1119± 32

Table 1: A summary of the mean input noise and spreads during the four main stages of testing. All values have been normalised to a module temperature of 0°C.

Table 1 gives a comparison of the mean values and spreads of the input noise for the main stages of testing for Endcap-A. All values of the input noise are comparable at each stage of testing. There is a slight increase in noise measurements taken in the cavern. This was the first time that the modules had been read out whilst being integrated within the TRT. This could be one reason for the small difference in values. For Endcap-C and the barrel, the results were similar. In general, there were no signs of module damage over the course of time.

D. *Thermal Performance*

The temperature of the module hybrid was monitored using a thermocouple placed directly on the hybrid surface. The connection of each module cooling block to the copper pipe circuit determines the quality of the module cooling. The spreads in module temperatures were minimal. The barrel had a $\sim$1 °C spread on temperatures during testing, and for the endcaps the spread was within 2 °C for each module type.

III. Cooling Problems

The ID evaporative cooling has had a history of problems since detector commissioning tests were performed at the beginning of 2007. Two major faults caused a significant loss of time to the ID test schedule. The first major fault involved the SCT heaters and the second was a fault with the external cooling plant. The problems and solutions will now be discussed.

A. Heaters

The first substantial tests of the evaporative cooling was in February 2007 during Barrel testing. Part-way through the tests a short occurred within the heater electrical connector supplying the power to the heaters. The role of the heater is to boil away any remaining C_3F_8 liquid in the cooling pipes as well as raising the temperature of the C_3F_8 above the cavern dew point. It is a small heating element put inside the cooling pipe at the exhaust. After an investigation, it appeared that moisture was getting into the connector. Consequently, all heaters were removed and re-fitted with a sleeve to prevent any more moisture getting in. However, just before the endcaps were due to be installed in May, the same heater fault occurred. A new heater layout was introduced to allow the continuation of detector installation whilst a solution was found for the heater failures. Nearly 120 heaters were moved to a more serviceable area, from the cooling exhausts at the SCT detector to the back of the cryostat flange. This allowed more accessibility for the repairs and future replacements of the heaters. New pipe work had to be re-engineered and then everything installed and leak tested. This re-work took til the end of 2007 to complete, allowing no cold testing of the SCT.

A solution has been made by re-designing the heater connector. The new designs have been installed and tested. Several new designs of heaters are also underway in case of future problems. A printed circuit instead of a coiled wire is one option, the other is a passive system that uses a hot liquid to heat up the cold C_3F_8 liquid from the detector. In addition, there were problems found with the heat exchangers, requiring more re-work. The connections were not leak tight and they all had to be removed, re-soldered, re-tested and installed and leak checked.

With both these solutions having been implemented, there have been no more faults, allowing the sign-off tests of both the barrel and endcaps to be finished.

B. Cooling Plant

After the sign-off tests of the barrel and endcap, the pixel commissioning was underway. In May 2008, subsequent cooling problems caused considerable delays to the schedule. Three out of six ID compressors failed catastrophically. The magnetic couplers slipped during the cooling start-up and were unable to drive the crank used to perform the compression. They also acted as a sealant of the C_3F_8 cooling volume from the motor and the compressor shaft. This caused the compressors to burn out as well as the loss of 100 kg of C_3F_8 from the system and the remaining 900 kg contaminated. Fortunately, only the cooling plant was affected and not the detector itself. A huge clean-up operation was implemented, involving the cleaning of the cooling plant as well as re-pairing of the compressors. The replacement of dirty pipe work was also necessary and additional filters were put in place.

The actual cause of this coupling slippage is still unknown, since an incomplete logging of data has made it difficult to come to an exact conclusion. However, sensors have been added to the system to detect any future slippage of the couplers. A C_3F_8 recovery tank has also been installed and tested, preventing any further losses in cooling liquid. Since then, the pipe work has been leak tested, new C_3F_8 has been introduced into the system and a successful commissioning of the cooling plant has been made. The pixel b-layer was cooled successfully during the ATLAS beam-pipe bake out, with the centre of the beam pipe reaching 220 °C. Better monitoring and logging of the cooling system will ensure a better understanding of the future replication of a fault.

IV. Cosmic Tests

For one week in March 2008, the SCT barrel participated for the first time in a global ATLAS "milestone" run, M6. Many of the sub-detector components were run during this week, allowing cosmic particles to be tracked from the SCT right through to the muon chambers. Cosmics provide an extremely useful method for testing the detector performance. Firstly they test the entire readout chain of the detector and its sub-components. Investigations into cross-talk between modules and noise resulting from synchronous running of the SCT and TRT barrels can also be investigated. They also test the alignment of the detector.

Most cosmic rays at sea level are muons with a mean energy of $\approx$ 4 GeV. Since the cosmic rays must pass through 100 m of concrete to access the cavern, the energies of the muons are expected to be much lower than those measured at sea-level. The cosmic muons entering the cavern, will do so predominantly via the two installation shafts, where there is no material for the cosmics to pass through. The angular spread of the cosmic rays is therefore limited affecting the frequency of cosmics passing through the SCT detector.

Three triggers were used during the M6 run. The tile calorimeter, the muon barrel resistive plate chambers, and an scintillator trigger specifically for the ID. Primarily the ID trigger was used, consisting of two scintillators placed above the muon chambers on level 8 in the ATLAS cavern. They were 144 cm $\times$ 40 cm $\times$2.5 cm and positioned $\sim$ 1 meter apart. Since the area of the scintillators is relatively small, a trigger rate of approximately 1 Hz was achieved.In order to have optimal charge collection efficiency it is essential to have a stable trigger time for the TRT and SCT detectors.

A. Timing

During beam physics, the SCT system clock will be synchronized to the bunch crossing clock cycle. However, for cosmics, the arrival of the particle is random within the system clock cycle. It is therefore necessary to measure the phase of the trigger with respect to the 40 MHz system clock. First, the clock and command signals of all the modules were synchronised to arrive at the same time. This is necessary, since compensation must be made for the different propagating delays of the signals from the timing electronics to the modules. Next, the SCT is timed in properly to ensure the readout of the correct event to maintain a synchronised Bunch Crossing ID (BCID). A course delay is initially varied (in 3 clock cycle steps) and a peak in the number of coincidences versus timing offset gives the approximate timing. For beam data, fine delay scans (280 ps level) will be used to optimise hit efficiencies.

B. *M6 Results*

During run 43719, more than 1200 tracks were present in the SCT, of which 1183 were present also in the TRT. They were reconstructed successfully by the reconstruction software. Figure 6 shows an example of a track going through the upper and lower parts of the SCT barrel.

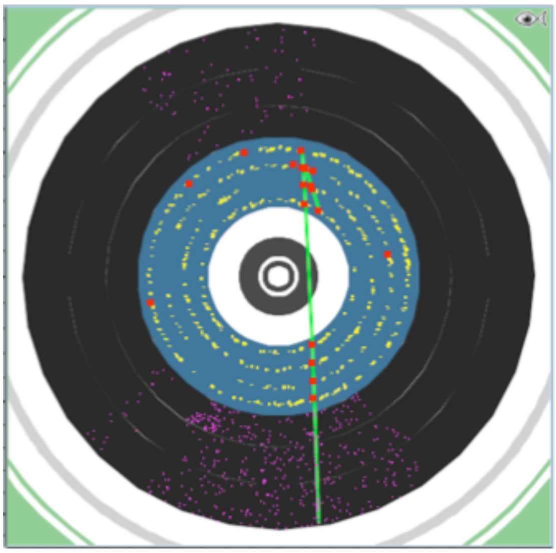

Figure 6: A cosmic muon going through the upper and lower sector of the barrel SCT.

Using the track parameters obtained from the reconstruction, a first estimate of the alignment between the TRT and SCT shows promising results. Without performing any alignment fits, a resolution of $-0.28 \pm 0.8mrad$ is found for the difference in phi measurements taken from the TRT and SCT ϕ track parameter. Residuals showing the difference between the x coordinate of the reconstructed track hit and the actual hit give values of 102 μm.

The noise occupancy was measured during cosmics run 43719. The results give an average module occupancy of 1.7×10^{-4}, well below the ATLAS specification of 5×10^{-4}.

V. Conclusions

The barrel and endcap SCT detectors are successfully installed in the ATLAS cavern. All modules and services have been tested and the detectors have officially been signed-off. The first steps towards global commissioning have begun, with the SCT joining their first milestone run in March, 2008. Cosmic rays have been tracked through the detector, testing the software and readout chain, as well as the module and track performance. Considerable delays have been caused due to faults within the ID cooling. However, these problems have now been solved and the SCT is due to resume the ATLAS global commissioning. Both beams were circulated in the LHC ring on September 10^{th}, with the SCT endcaps biased at 20 V. Events were recorded in the detector with both endcaps glowing from beam halo muons. The SCT looks forward to its first collisions next year.

References

[1] The ATLAS experiment at the CERN Large Hadron Collider", JINST, A53, 384-407, (2008)

[2] The LHC Conceptual Design Report - The Yellow Book, CERN/AC/95-05(LHC) (1995)

[3] A. Abdesselam *et al.*, The barrel modules of the ATLAS semiconductor tracker, NIM A 568: 642-671 (2006)

[4] A. Abdesselam et al., The ATLAS semiconductor tracker end-cap module, NIM A 575: 353-389 (2007)

[5] A. Ahmad *et al.*, The silicon microstrip sensors of the ATLAS semiconductor tracker, NIM A 578: 98-118 (2007)

[6] F. Campabadal *et al.*, Design and performance of the ABCD3TA ASIC for readout of silicon strip detectors in the ATLAS semiconductor tracker, NIM A 552: 292-328 (2005)

[7] A. Adesselam *et al.*, The optical links of the ATLAS SemiConductor Tracker, JINST 2 P09003 (2007)

[8] B. M. Demirkoz, ATLAS SCT collaboration, Cosmic tests and performance of the ATLAS semiconductor tracker barrels, NIM A 572: 43-47 (2007)

[9] A. Adesselam *et al.*, The Integration and Engineering of the ATLAS SemiConductor Tracker Barrel, submitted to JINST(2008)

[10] A. Adesselam *et al.*, The data acquisition and calibration system for the ATLAS Semiconductor Tracker, JINST 3 P01003 (2008)